Cumulative geomagnetic disturbances modulate global photosystem stoichiometry through temperature-dependent gating

Andrey V. Kitashov [1,2]

[1] Faculty of Biology, Shenzhen MSU-BIT University, Shenzhen 518100, China [2] Faculty of Biology, Lomonosov Moscow State University, Leninskie Gory, Moscow 119991, Russia

Preprint DOI: https://doi.org/10.64898/2026.02.17.706448 **Version**: March 14, 2026 (v3) **Cite as**: Kitashov, A. V. (2026). bioRxiv 2026.02.17.706448, version 3; doi: 10.1101/2026.02.17.706448

---

1. Abstract

Space weather exerts profound effects on Earth's technological systems, yet its influence on the terrestrial biosphere remains largely unexplored at the global scale. Despite decades of research on solar–terrestrial interactions, most studies have focused on technological and atmospheric effects, while potential influences on biological regulation remain largely unexplored. While local experiments suggest magnetic sensitivity in plants (Galland and Pazur 2005; Belyavskaya 2004), observational evidence for a planetary-scale vegetative response to geomagnetic disturbances is lacking. In particular, it is unclear whether weak and intermittent geomagnetic disturbances can leave detectable signatures in ecosystem-scale physiological processes.

Here, we analyze a decade of satellite-derived solar-induced chlorophyll fluorescence (SIF) data alongside geomagnetic indices to isolate non-seasonal physiological anomalies. Using temperature-stratified cumulative correlation analysis and multivariate models controlling for radiative and hydrological drivers, we identify a robust, cumulative, and thermally gated association between geomagnetic activity and vegetation fluorescence.

We report a global-scale coherent modulation of photosystem balance, potentially inferred from the SIF_{757}/SIF_{771} ratio, with recurrent geomagnetic disturbances, exhibiting maximal coherence under cold and moderate thermal conditions and weakening under `Optimum` and `Warm Stress` regimes. This response intensifies with increasing integration window length, indicating progressive physiological integration of repeated perturbations. Comparative analyses demonstrate that geomagnetic forcing is frequently comparable to or exceeds major climatic drivers in explaining fluorescence variability within biologically active regimes.

We propose a mechanism consistent with magnetic modulation of radical pair spin dynamics in iron–sulfur clusters and cryptochromes, potentially influencing reactive oxygen species generation and redox-regulatory adaptation. Our findings suggest that plants have evolutionarily co-opted geomagnetic variability as an informational signal, integrating it into existing redox-regulatory networks. Rather than a passive mechanical perturbation, the observed response reflects an evolved sensitivity that operates near physiological criticality—a hypothesis that opens new frontiers in understanding magnetosphere–biosphere coupling.

Keywords: geomagnetic activity, solar-induced chlorophyll fluorescence (SIF), plant stress physiology, temperature-dependent regulation, cumulative environmental forcing, photosynthetic redox balance, magnetosphere–biosphere coupling, space weather impacts, evolutionary co-option, biological information processing

2. Introduction

Whether large-scale space weather variability can influence biological regulation on Earth remains among the least explored questions in Earth system science. Although geomagnetic storms are well known for disrupting satellites and power grids, their potential role as subtle modulators of physiological processes in living systems has received little systematic attention. While magnetic fields are known to influence navigation in birds *via* cryptochromes (Wiltschko and Wiltschko 2019; Xu et al. 2021), plants remain largely considered "blind" to geomagnetic fields in the context of gross primary production. However, recent evidence suggests that cryptochromes in plants may have retained or co-opted similar magnetosensitivity mechanisms (Mattei and Hore 2014; Galland and Pazur 2005; Nordmann, Hochstoeger, and Keays 2022). Recent experimental studies have documented magnetic field effects on plant growth, gene expression,

and stress responses (Belyavskaya 2004; Parmagnani and Maffei 2022). We therefore hypothesize that weak geomagnetic disturbances can exert detectable cumulative effects on photosynthetic regulation under specific physiological conditions, particularly under cold-induced sink limitation and associated redox imbalance.

To interpret any statistical association between geomagnetic activity and vegetation dynamics, it is essential to clarify whether plausible physical and biochemical coupling mechanisms exist. The physical basis for such sensitivity likely involves the radical pair mechanism, where weak magnetic fields modulate the spin dynamics of short-lived radical pairs (Hore and Mouritsen 2016). In photosynthetic organisms, potential targets include not only cryptochromes but also iron–sulfur (Fe–S) clusters within the electron transport chain (Parmagnani and Maffei 2022). From an evolutionary perspective, the ubiquity of magnetosensitive elements in core metabolic machinery—Fe–S clusters, radical-pair intermediates, and cryptochromes—raises the possibility that sensitivity to geomagnetic variability is not an accident but an ancient and conserved feature of biological systems. Plants may have evolved to perceive geomagnetic fluctuations not as noise, but as an informational layer of their environment, integrating it into existing redox-regulatory networks that govern stress responses and acclimation (Johnsen and Lohmann 2005; Meert et al. 2016).

Even if biological sensitivity exists, detecting it in observational data is nontrivial. The main methodological challenge lies in the temporal scale disparity between instantaneous magnetic events and physiological responses, which are expected to integrate repeated weak perturbations over days to weeks through regulatory and buffering processes. Magnetic disturbances occur on timescales ranging from minutes to days, whereas photosynthetic acclimation and stress responses operate through hierarchical regulatory networks spanning hours to weeks, and extending into seasonal and life-cycle scales. Resolving such multi-scale even week-range interactions requires analytical approaches capable of detecting cumulative and condition-dependent effects rather than isolated transient responses.

To bridge this gap, we utilize satellite SIF data, which has established itself as a robust proxy for gross primary production and photosynthetic regulation (Guanter et al. 2014; Frankenberg et al. 2011). Remote sensing of SIF has been comprehensively reviewed, including retrieval approaches, limitations, and physiological interpretation across spatial and temporal scales (Meroni et al. 2009; Mohammed et al. 2019). Because SIF responds sensitively to changes in the redox state and energy dissipation pathways of the photosynthetic apparatus (Samuilov et al. 1998), it provides a unique window into physiological perturbations that may not be captured by conventional vegetation indices.

Here we combine temperature-stratified cumulative correlation analysis with multivariate controls for radiative and hydrological drivers to identify distinct global patterns of SIF modulation by geomagnetic disturbances. Long-term satellite SIF products provide consistent global constraints on photosynthetic variability and have been benchmarked against ecosystem carbon exchange across diverse biomes (Mohammed et al. 2019). By applying harmonic regression, temperature stratification, and multivariate screening to a decade-long dataset, we distinguish genuine physical signals from spurious correlations driven by seasonality and environmental confounding. This framework enables a systematic assessment of whether weak geomagnetic variability can be integrated into photosynthetic regulation at ecosystem scale under specific physiological constraints.

To our knowledge, this represents the first global-scale, physiologically stratified assessment of cumulative geomagnetic effects on terrestrial photosynthesis.

3. Results

We first address the most basic question: whether detrended SIF residuals (after removal of seasonal cycles and long-term trends) show any systematic association with geomagnetic activity that scales with integration window length.

Signal Robustness and Spatiotemporal Structure

A statistically significant correlation alone is insufficient to establish biological relevance. To distinguish potential biophysical coupling from instrumental noise and environmental confounding, we examined the multi-scale association between SIF anomalies and geomagnetic forcing across four geographic scenarios (Fig. 1), focusing on spatial contrasts, temperature dependence, and integration-window scaling. Under a purely instrumental artifact, we would expect either (i) amplification in the SAA, or (ii) no consistent temperature dependence, and no reproducible window-dependent morphology across vegetated regions.

The abiotic control (`Sahara`, Fig. 1D) and the high-radiation South Atlantic Anomaly (`SAA`, Fig. 1C) are dominated by stochastic variability, characterized by wide confidence intervals and intermittent statistical significance. The ab-

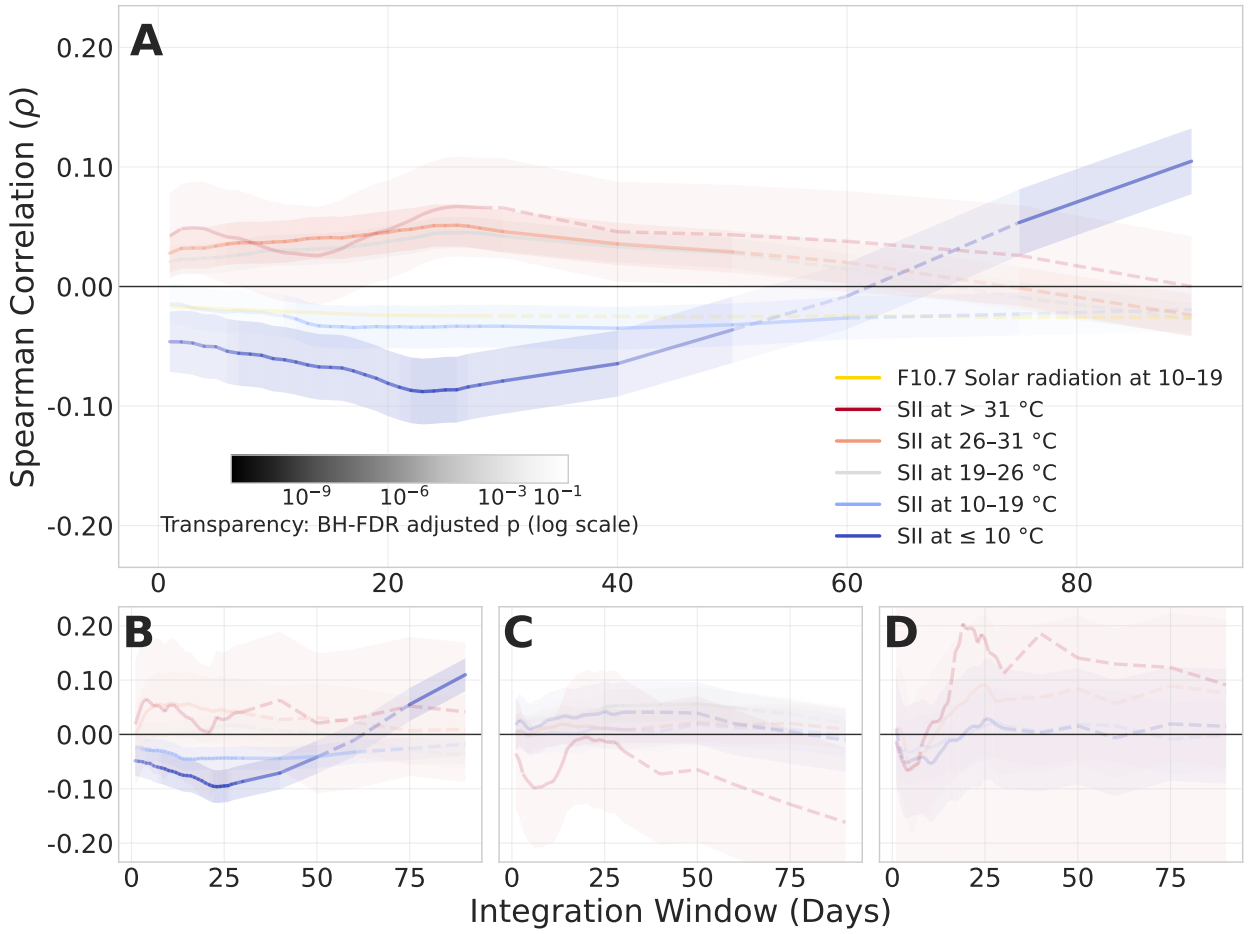

Figure 1: **Temperature-dependent cumulative response of vegetation fluorescence to geomagnetic activity.** Spearman's rank correlation coefficients (ρ) between detrended SIF at 771 nm and the cumulative Storm Intensity Index (SII = $-Dst$, Disturbance Storm Time Index) are shown across integration windows up to 90 days, evaluated on a predefined sparse grid (1–28 daily, plus 30, 40, 50, 60, 75, and 90 days). SII is expressed as a cumulative moving-average forcing over a window of length *w* days, used as a proxy for repeated disturbances integrated by physiology. Panels compare biologically active ecosystems—(A) `Global High-LAI` and (B) `Control North`—with instrumental and abiotic controls—(C) `SAA` and (D) `Sahara` (see Supplementary Table S1 and Fig. S9). Curves are stratified by ambient temperature, defined from a fixed moving-average temperature context window and used for physiological binning. Shaded regions indicate 95% confidence intervals. Line style and opacity encode statistical significance (p-values first corrected for autocorrelation using effective sample size and subsequently FDR-adjusted across integration windows within each temperature bin), where autocorrelation correction replaces the nominal sample size by an effective sample size, reducing false positives in strongly smoothed time series. The gold curve in (A) shows the correlation with F10.7 cm solar radio flux for a representative thermal bin; F10.7 correlations are qualitatively nearly identical across temperature bins (Supplementary Fig. S1). To further separate geomagnetic from direct solar influences, we compared the attribution of SIF variability to SII versus F10.7 across the `Control North` region (Supplementary Fig. S2), confirming that the observed effects are primarily associated with magnetospherically mediated disturbances rather than direct solar irradiance. Qualitatively comparable but weaker patterns are observed for SIF wavelengths 740 and 757 nm and for the SIF_{757}/SIF_{771} stress indicator (Supplementary Figs. S3–S5).

sence of a coherent window-dependent structure in these controls provides no evidence for systematic retrieval artifacts associated with energetic particle precipitation.

To assess potential solar and radiative confounding, we overlaid correlations with solar radio flux (F10.7) in the global analysis (Fig. 1A). Across integration windows, F10.7 exhibits a weaker response and most importantly lacks the cumulative structure observed for geomagnetic forcing, indicating that the detected signal is unlikely to be explained by concurrent solar variability alone. F10.7 captures broad solar variability and irradiance-related covariation (Tapping 2013), whereas the geomagnetic index represents magnetospherically mediated disturbances.

In contrast, biologically active ecosystems (`Global High-LAI` and `Control North`) exhibit narrow confidence intervals and consistently high statistical significance. The Northern Hemisphere `Control North` analysis (Fig. 1B) reveals a pronounced temperature-dependent morphology: a cumulative negative association confined to cold thermal regimes (<12 °C), peaking at integration windows of approximately 20–30 days. This structure is partially smoothed in the global aggregate, consistent with spatial averaging across heterogeneous climatic regimes.

The biophysical origin of the signal is supported by the robust cumulative response observed in the `Global High-LAI` and `Control North` regions (Fig. 1A,B), which contrasts sharply with the absence of such patterns in the radiation-intense `SAA` and the barren `Sahara` (Fig. 1C,D). Crucially, if the observed anomalies were driven by particle-induced sensor noise, the correlation would be most pronounced within the `SAA` due to the significantly higher particle flux (Schaefer et al. 2016; Crisp et al. 2017). The lack of such amplification in the `SAA`, combined with the strong signal in radiation-stable vegetated regions, disfavors instrumental artifacts as the primary driver of the observed phenomenon.

In addition, correlations between SII and major environmental drivers (PAR, VPD, and cloud cover) were uniformly weak across all scenarios and integration windows ($|\rho| < 0.05$), indicating that the observed SIF–SII coupling is not mediated by concurrent meteorological variability.

Consistent with this interpretation, analogous analyses of individual SIF wavelengths (740, 757 nm) and the stress-sensitive spectral index (SIF_{757}/SIF_{771}) reveal qualitatively similar but systematically weaker cumulative patterns (Supplementary Figs. S3–S5). By contrast, the far-red 771 nm channel, located at the long-wavelength tail of the fluorescence emission spectrum and preferentially associated with Photosystem I, exhibits enhanced sensitivity to redox imbalance and acceptor-side limitation (Porcar-Castell et al. 2014; Cendrero-Mateo et al. 2015), consistent with its stronger and more coherent cumulative response (Fig. 1).

Having established a coherent, window-dependent signal that is absent in non-biological controls, we next quantified how its magnitude compares with that of established climatic drivers across temperature regimes (Fig. 2).

Comparative statistical screening further supports this interpretation by revealing a strong thermal modulation of signal efficacy. In the `Optimum` thermal regime, geomagnetic forcing (SII) systematically outperforms solar irradiance (F10.7), exhibiting superior explanatory power. The cumulative signal strength in the `Optimum` regime, quantified by the area under the correlation spectrum (AUC), is approximately 19-fold higher for SII relative to F10.7 (AUCratio ≈ 19.3). AUC summarizes the cumulative association across the tested window grid and is used here as an integrated effect-size proxy rather than a formal model selection criterion. AUC is used to summarize the spectrum across windows without focusing on a single window.

Under `Extreme Heat` conditions, this contrast sharply declines (AUCratio ≈ 0.9) and becomes indistinguishable from stochastic variability, consistent with thermal modulation of the underlying coupling mechanism.

Driver dominance across temperature regimes

This pattern is further illustrated in Fig. 2, which summarizes the relative magnitude of associations between SIF stress anomalies and cumulative SII, PAR, and VPD across temperature regimes.

Here, the stacked $|\rho|$ spectra provide a descriptive comparison of association strength across timescales; they do not imply causality, but indicate whether geomagnetic forcing is competitive with canonical drivers within the same physiological regime. Each bar reflects a scenario-level (mask-pooled) rank association computed within the corresponding temperature regime, rather than a spatial average of per-pixel correlations.

Across most analyzed SIF spectral channels, geomagnetic forcing exhibited detectable associations with vegetation fluorescence that were comparable in magnitude to those of major climatic drivers, including PAR and VPD. This

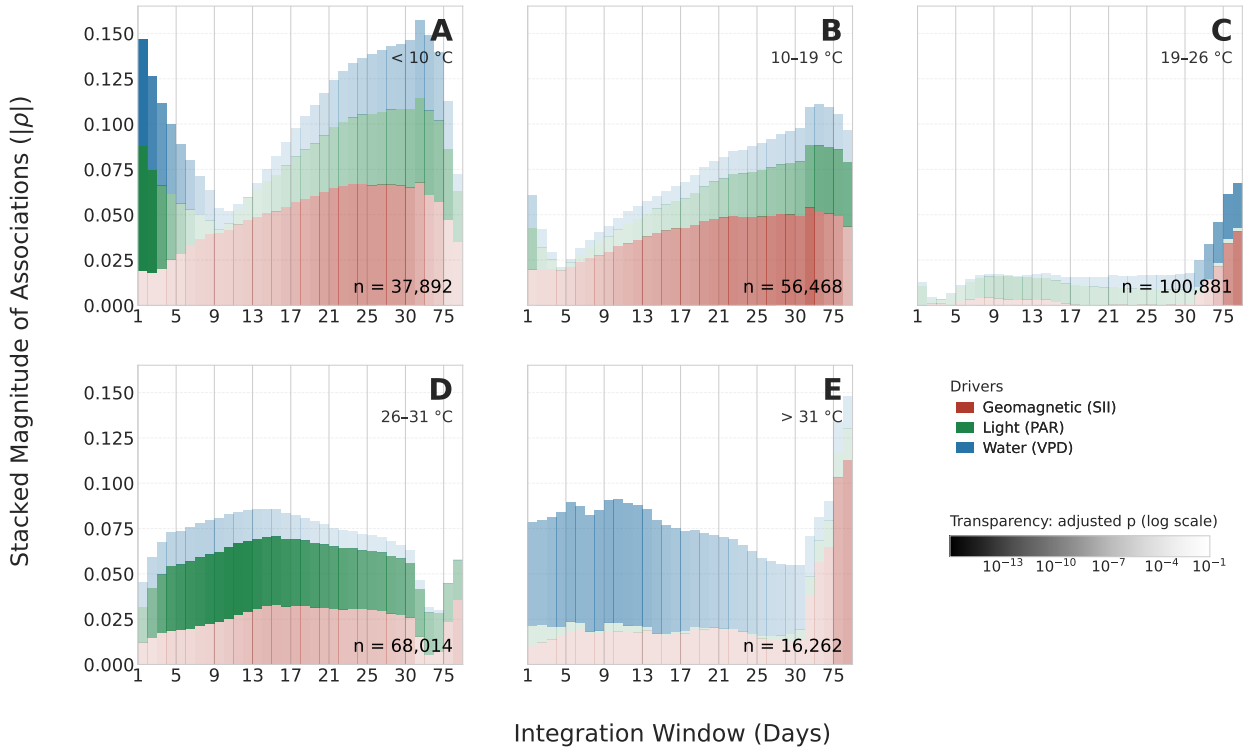

Figure 2: **Relative dominance of geomagnetic versus climatic drivers across timescales and temperature regimes.** Stacked spectra summarize the magnitude of associations between detrended fluorescence stress anomalies (SIF_{757}/SIF_{771}) and three drivers—geomagnetic forcing (SII), radiative forcing (Photosynthetically Active Radiation, PAR), and atmospheric dryness (Vapor Pressure Deficit, VPD)—across integration windows (as in Fig. 1) for the `Global High-LAI` scenario. For each scenario and temperature regime, ρ is computed on the pooled spatiotemporal sample within the scenario mask (i.e., aggregating all valid grid-cell–day observations), yielding a single scenario-level association per driver and integration window rather than pixel-wise estimates. For each temperature regime (A–E; `Cold` to `Extreme Heat`), bars show absolute Spearman correlations (|ρ|) at each integration window, stacked by driver (SII in red, PAR in green, VPD in blue). Bar opacity encodes statistical significance (p-values first corrected for autocorrelation using effective sample size and subsequently FDR-adjusted across integration windows within each temperature bin; legend in panel F). Corresponding spectra for other scenarios are shown in Supplementary Figs. S6–S8.

pattern was consistently observed across multiple geographic scenarios and temporal integration windows, as confirmed by representative supplementary analyses.

However, the strength, coherence, and thermal specificity of the cumulative response were markedly enhanced for the stress-sensitive spectral index (SIF_{757}/SIF_{771}). This metric exhibited superior signal-to-noise ratio, reduced sensitivity to radiative variability, and more stable window-dependent structure, thereby enabling a more direct physiological interpretation of the observed associations and motivating its central role in subsequent dominance and robustness analyses (Figs. 2–3).

The preferential amplification of geomagnetic associations in the stress index, which reflects photochemical regulation and non-photochemical quenching, is consistent with a physiological modulation of photosynthetic efficiency under geomagnetic disturbance. Although the underlying mechanisms remain uncertain, this pattern suggests an interaction between geomagnetic activity and plant stress-response pathways.

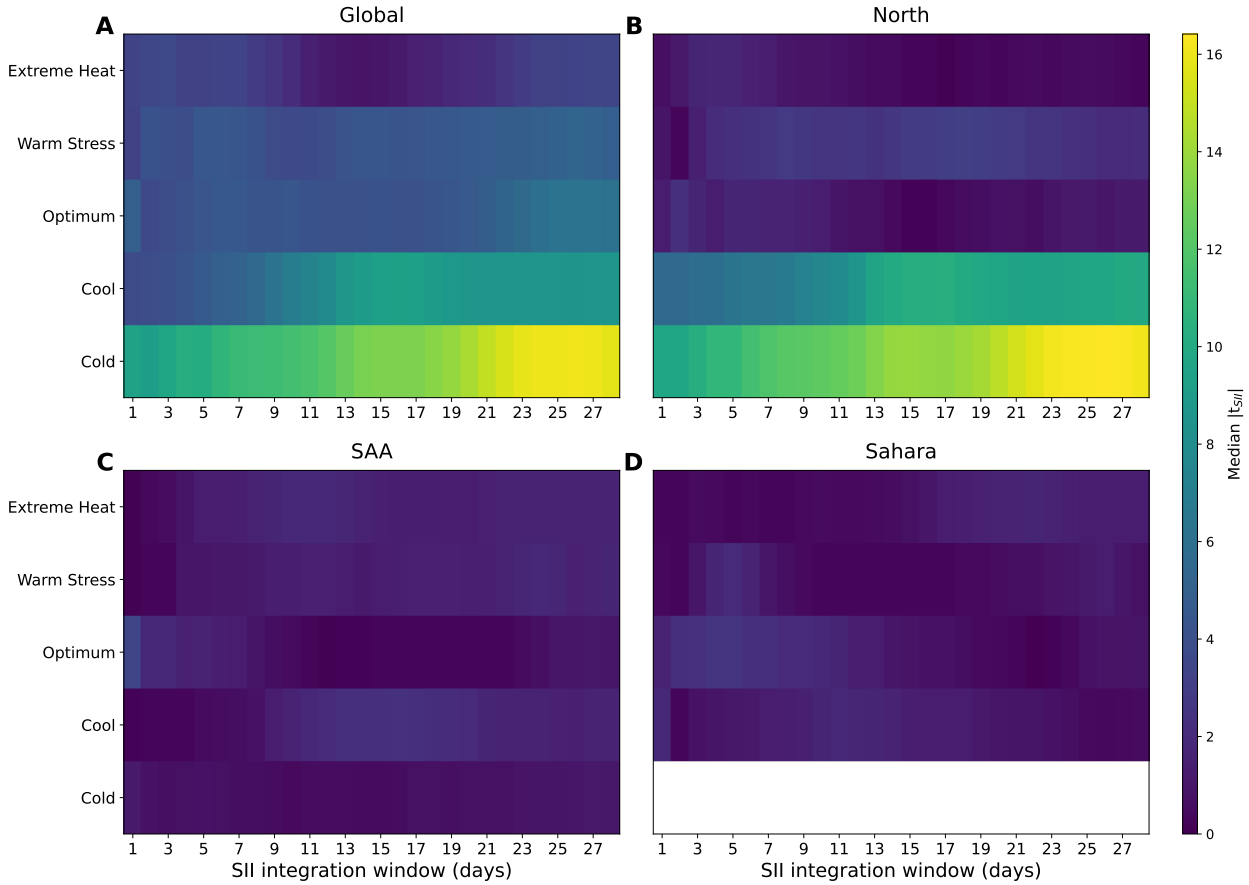

Figure 3: **Robustness landscapes of the SIF-geomagnetic coupling across geographical scenarios.** Heatmaps show the absolute t-statistic ($|t_{SII}|$) for the SII coefficient in a multivariate model ($SIF_{resid} \sim SII + PAR + VPD$) at 771 nm. Values represent the median across all tested combinations of environmental integration windows (PAR, VPD) for each temperature bin and SII window, thereby emphasizing robust partial SII effects over specific model configurations. Hence, warmer colors indicate stronger partial effects of geomagnetic forcing after accounting for PAR and VPD. **(A)** Global vegetated areas (High LAI) showing a broad region of significant association at integration windows of 15–25 days. **(B)** Northern Hemisphere control region (NA & Eurasia) showing consistent coupling patterns. **(C)** South Atlantic Anomaly (SAA) scenario; the absence of dominant signals similar to (A) suggests that sensor-particle interactions are not the primary driver of the observed global trend. **(D)** Sahara Desert (Barren land) as a negative biophysical control, showing a lack of organized response (this control lacks `Cold` data). All panels use a shared color scale and 0.5° spatial resolution. The absence of warm colors in (C) and (D) confirms that the signal is specific to vegetated regions.

Finally, to isolate the partial geomagnetic contribution from environmental covariation and to test robustness beyond pairwise correlations, we performed an exhaustive multivariate matrix search across four geographical scenarios (Fig. 3). For each temperature bin and SII integration window, we summarize the distribution of partial SII t-statistics across all tested environmental window combinations using the median. The results demonstrate that the strongest statistical signals ($|t_{SII}| > 4$) are concentrated in vegetated regions (Fig. 3A, B) and are characterized by a specific temporal fingerprint: a cumulative effect that peaks at integration windows after approximately 20 days. This "accumulation memory" is consistent with physiological gating mechanisms rather than instantaneous physical interference. Crucially, the analysis of the `SAA` (Fig. 3C)—a region known for high ionizing radiation flux that could induce instrumental noise in the OCO-2 (Orbiting Carbon Observatory-2) spectrometers—did not reveal a structured response landscape comparable to the global vegetated signal (Heirtzler 2002; Schaefer et al. 2016; Crisp et al. 2017). Similarly, the `Sahara` barren scenario (Fig. 3D) yielded no significant associations, confirming that the SII effect requires the presence of active photosynthetic machinery. The stability of the signal across the Northern Hemisphere control (Fig. 3B) further reinforces the conclusion that the observed geomagnetic influence is consistent with a large-scale biophysical signal and is robust to local climatic variations and instrumental anomalies. We emphasize that this analysis is used to assess robustness and biological plausibility (e.g., contrast with SAA/Sahara), rather than to provide the primary basis for statistical inference.

Together, these results confirm that geomagnetic forcing exerts a statistically robust, cumulative, and physiologically structured influence on vegetation fluorescence that cannot be explained by concurrent radiative or hydrological variability alone.

Surrogate tests based on permutation of geomagnetic years indicate that the observed cumulative SII–SIF correlations approach or exceed the upper range of surrogate realizations (Supplementary Fig. S10).

4. Discussion

Summary of main findings

The central result of this study is the detection of a cumulative, temperature-dependent association between geomagnetic disturbances and vegetation fluorescence at the global scale. This finding raises two immediate questions: why the effect is strongest under cold conditions, and through which physiological pathways such weak forcing could operate. The effect is strongest under `Cold` and `Cool` regimes, peaks at integration windows of approximately 20–30 days, and weakens under `Optimum` and `Warm Stress` and further under `Extreme Heat` conditions, with maximal coherence and dominance observed in the stress-sensitive $\mathrm{SIF}_{757}/\mathrm{SIF}_{771}$ index. Instrumental and abiotic controls show no comparable structure (Fig. 1C,D). While comparison with key climatic drivers—PAR and VPD—reveals that geomagnetic forcing dominates the association spectrum specifically under cool conditions (Fig. 2B–C). Direct solar forcing (F10.7) exhibits weak and incoherent associations, and its correlations are nearly identical across temperature bins (Supplementary Fig. S1).

These convergent lines of evidence indicate that the observed signal reflects a biologically mediated response rather than radiative, climatic, or instrumental artifacts. Importantly, the cumulative structure of the signal suggests that the underlying mechanism is not impulsive. Instead, it operates through integration across repeated perturbations. This pattern implies the involvement of regulatory and redox-buffering pathways rather than direct photophysical disruption alone.

Thermal modulation and sink limitation

Photosynthetic performance is strongly constrained by the kinetic mismatch between temperature-insensitive photochemical reactions and temperature-dependent biochemical carbon fixation. Notably, the strongest geomagnetic associations consistently emerge at integration windows of approximately 20–30 days (Fig. 1), indicating that the underlying mechanism operates through physiological buffering and cumulative redox imbalance rather than through instantaneous perturbations. Primary charge separation and electron transport exhibit low thermal sensitivity ($Q_{10} \approx 1.0$) (Ensminger, Busch, and Huner 2006), whereas Rubisco carboxylation and Calvin–Benson cycle turnover display much higher temperature dependence ($Q_{10} \approx 2$–3) (Sage and Kubien 2007; Yamori, Hikosaka, and Way 2014).

Under low-temperature conditions, this mismatch leads to sink limitation, accumulation of reducing equivalents, and over-reduction of the photosynthetic electron transport chain (Huner, Öquist, and Sarhan 1998; Tikkanen and Aro 2014).

Although plants have evolved multiple protective and compensatory mechanisms operating across different temporal scales—including rapid non-photochemical quenching and xanthophyll cycling (Demmig-Adams and Adams 1996; Müller, Li, and Niyogi 2001), intermediate regulation *via* cyclic electron flow and alternative sinks (Munekage et al. 2004; Shikanai 2014), and longer-term adjustments in photosystem stoichiometry and antenna organization (Anderson, Chow, and Park 1995; Walters 2005)—these responses cannot fully eliminate transient excitation pressure under persistent cold stress.

Our temperature stratification is based on daily and multi-day mean values, which integrate pronounced diurnal variability. In the `Cool` regime in particular, plants are frequently exposed to nocturnal or early-morning temperatures approaching or falling below freezing, followed by near-optimal daytime conditions. Such rapid thermal oscillations preclude full physiological and epigenetic acclimation (Way and Yamori 2014; Atkin and Tjoelker 2003). As a result, photosynthetic machinery remains in a quasi-transitional state characterized by recurrent redox imbalance.

This recurrent redox tension defines a physiological window of sensitivity in which long-lived reduced intermediates accumulate and reaction kinetics slow. Under these conditions, weak external perturbations can exert a measurable influence. Cold-induced sink limitation therefore enhances excitation pressure at photosystem I and prolongs the lifetime of reduced acceptor-side components, increasing the susceptibility of the system to subtle magnetic modulation.

As temperature approaches the physiological optimum for C3 photosynthesis (approximately 25 °C), enzymatic turnover accelerates and redox balance is restored (Kumarathunge et al. 2019). Under these conditions, excitation pressure decreases and the geomagnetic signal progressively dissipates into background physiological variability. It becomes effectively masked by dominant metabolic fluxes.

By contrast, high-temperature stress primarily affects photosynthesis through enzyme destabilization, membrane perturbation, and large-scale metabolic and whole-plant physiological reprogramming (Sharkey 2005; Yamori, Hikosaka, and Way 2014). These processes operate at higher levels of systemic organization and are dominated by strong thermal and oxidative constraints. As a consequence, the relative contribution of weak magnetic effects is reduced. Although heat represents a severe stress condition, it fails to sustain the specific redox and kinetic environment required for magnetic sensitivity. In this sense, cold stress exposes a redox-controlled biophysical regime, whereas heat stress primarily reorganizes whole-plant physiology at scales where spin-dependent perturbations are comparatively negligible.

Sensitivity of Photosystem I acceptor-side processes

To translate the observed statistical patterns into physiological terms, we now consider which components of the photosynthetic apparatus are most likely to mediate geomagnetic sensitivity. Photosystem (PS) I is particularly vulnerable to acceptor-side limitation and photoinhibition under conditions of redox imbalance (Sonoike 2011; Tiwari et al. 2016). Over-reduction of Fe–S clusters (F_X, F_A, F_B) and impaired electron export increase susceptibility to oxidative damage and modify electron-transfer kinetics (Tikkanen and Aro 2014).

Iron–sulfur clusters are central components of many biological electron-transfer systems in which spin-dependent radical-pair intermediates have been implicated in magnetic-field sensitivity. Experimental and theoretical studies in non-photosynthetic systems have demonstrated that Fe–S–associated redox reactions can participate in magnetically modulated radical-pair dynamics (Rodgers and Hore 2009; Hore 2016; Evans and Hore 2013). Although direct evidence for such effects in photosystem I is currently lacking, the presence of long-lived reduced intermediates under stress conditions suggests a physically plausible interface for weak magnetic perturbations.

Numerous studies demonstrate that PSI redox regulation plays a central role in coordinating photoprotection and metabolic demand (Pfannschmidt et al. 2009; Tikkanen and Aro 2014). The preferential sensitivity of the 771 nm fluorescence channel in our data is consistent with perturbations localized to PSI and far-red emission.

The enhanced coherence and dominance of the $\mathrm{SIF}_{757}/\mathrm{SIF}_{771}$ stress index further indicate a redistribution of excitation energy between the two photosystems and a coordinated adjustment of light-harvesting and energy-dissipation pathways. Such spectral rebalancing is consistent with physiological analyses linking far-red fluorescence ratios to dynamic redistribution of excitation energy and regulation of photosystem stoichiometry (Porcar-Castell et al. 2014; Cendrero-Mateo et al. 2015).

Radical-pair dynamics and magnetic compatibility

Any mechanistic interpretation must ultimately be compatible with known physical principles governing electron-transfer reactions in proteins. Charge separation and recombination in photosynthetic reaction centers generate short-lived radical pairs whose spin dynamics can be influenced by weak magnetic fields (Rodgers and Hore 2009; Hore 2016). Experimental and theoretical studies have established the physical plausibility of magnetic modulation of singlet–triplet interconversion in biological systems, including photosynthetic complexes (Ritz, Adem, and Schulten 2000; Evans and Hore 2013).

Although direct measurements of geomagnetic sensitivity in PSI are scarce, the presence of long-lived radical intermediates under acceptor-side limitation suggests compatibility with radical-pair mechanisms. Our results are therefore consistent with, though not direct evidence for, magnetic modulation of reaction-center dynamics.

Iron–sulfur centers are also present in the cytochrome b6f complex, where the Rieske protein plays a pivotal regulatory role in controlling electron flux and excitation balance between the two photosystems (Kurisu et al. 2003; Stroebel et al. 2003). Because b6f represents a major kinetic bottleneck within the photosynthetic electron transport chain, perturbations at this level may propagate system-wide effects on energy distribution and redox signaling.

Rieske-type Fe–S proteins belong to a widespread family of redox-active cofactors involved in central metabolic intersections across prokaryotes and eukaryotes (Imlay 2006). Their recurrent involvement in spin-dependent redox reactions supports the plausibility of radical-pair–mediated magnetic sensitivity as a general physical interface between weak magnetic fields and metabolism.

Within this framework, the radical-pair mechanism represents one of the most extensively developed candidates for biological magnetoreception (Hore 2016; Ritz, Adem, and Schulten 2000). Although originally formulated in the context of animal navigation, its underlying principles are directly applicable to photosynthetic and redox-active protein complexes. Our observations are therefore compatible with a scenario in which geomagnetic perturbations subtly modulate radical-pair dynamics within PSI and b6f-associated pathways, thereby influencing downstream regulatory processes.

ROS-mediated amplification and photoprotective signaling

Perturbations of PSI electron transport enhance electron leakage to molecular oxygen, generating superoxide ($O_2^{\bullet -}$) and hydrogen peroxide (H_2O_2) (C. H. Foyer and Noctor 2005; Apel and Hirt 2004). The progressive strengthening of geomagnetic effects with increasing integration window length (Figs. 1 and 3) suggests that such redox perturbations are repeatedly accumulated and integrated within cellular regulatory networks. Photosystem II also represents a major source of singlet oxygen (^1O_2), particularly under conditions of excitation imbalance and impaired electron flow at the QB site (Krieger-Liszkay 2005; Pospíšil 2016). Additional redox-active components in the chloroplast stroma and thylakoid membrane further contribute to ROS production.

The observed suppression of SIF under geomagnetic disturbances likely reflects a rapid systemic adjustment to oxidative stress. Elevated levels of reactive oxygen species (ROS), particularly hydrogen peroxide, are known to act as potent inhibitors of the photosynthetic machinery. Experimental evidence indicates that H_2O_2 accumulation directly suppresses photosynthetic electron transport in the Hill reaction and inhibits the activity of both PSII and PSI (Samuilov et al. 2001). Such direct biochemical inhibition, coupled with the magnetic modulation of radical pair dynamics, suggests that the geomagnetic signal in SIF represents a real-time proxy for the redox state of the photosynthetic apparatus rather than a simple phenological shift.

Beyond the chloroplast, the mitochondrial electron transport chain constitutes another major and dynamically regulated source of superoxide (Rhoads and Subbaiah 2006; Møller, Jensen, and Hansson 2007). Crosstalk between chloroplast and mitochondrial redox states coordinates cellular energy balance and stress signaling.

These multiple ROS sources are closely coupled to primary charge-separation and recombination reactions involving radical-pair intermediates. Perturbations of spin-dependent reaction pathways may therefore influence both electron-transfer kinetics and the probability of ROS formation at multiple redox-sensitive sites.

ROS occupy a dual functional role in plant physiology. At high concentrations, they cause oxidative damage to proteins, lipids, and nucleic acids. At controlled levels, they act as central signaling molecules regulating acclimation, gene expression, and metabolic reconfiguration (C. H. Foyer and Noctor 2005; Suzuki et al. 2006; Mittler et al. 2011).

This duality is widely discussed as reflecting an evolutionary shift in which reactive by-products of aerobic metabolism, initially dominated by damaging effects, were progressively incorporated into regulated signaling circuits (C. Foyer and Noctor 2009; Noctor, Reichheld, and Foyer 2018). In this view, oxidative stress responses gradually developed into information-processing modules capable of integrating environmental variability.

Redox perturbations originating in PSI, PSII, or mitochondria can therefore be transduced into coordinated regulatory responses through interconnected signaling networks (Rhoads and Subbaiah 2006; Møller, Jensen, and Hansson 2007; Noctor, Reichheld, and Foyer 2018). Subtle shifts in electron-transfer probabilities, including those potentially influenced by magnetic-field–dependent radical-pair modulation, may alter ROS formation rates across multiple sites (Hore 2016; Evans and Hore 2013).

From this perspective, ROS signaling provides a plausible channel of magnetic sensitivity within redox-regulatory networks that operates in parallel with Fe–S–associated mechanisms. Weak magnetic perturbations may bias existing redox-sensitive pathways that have been optimized to detect small deviations from homeostasis (Mittler et al. 2011; C. Foyer and Noctor 2009). Magnetically induced redox fluctuations may therefore be interpreted as inputs into pre-existing regulatory architectures governing stress perception and acclimation (Noctor, Reichheld, and Foyer 2018; Suzuki et al. 2006).

Cryptochromes as integrative regulatory nodes

Cryptochromes are flavoproteins that have undergone evolutionary specialization for light-dependent redox cycling involving radical intermediates and exhibit magnetic sensitivity *in vitro* and *in vivo* (Ritz et al. 2004; Ahmad et al. 2016). The first systematic evidence for plant magnetoreception came from studies showing magnetic field effects on germination and early seedling development (Galland and Pazur 2005). Subsequent ultrastructural analyses revealed that magnetic fields can alter calcium homeostasis and cellular organization in root meristems (Belyavskaya 2004).

In plants, cryptochromes have so far been shown to regulate antioxidant capacity, stomatal conductance, circadian rhythms, and stress-responsive gene expression. These functions suggest a primary role in coordinating cellular redox state with environmental light cues (Chaves et al. 2011; Cosentino et al. 2019). A recent comprehensive review synthesizes the current understanding of plant magnetoreception, emphasizing the central role of cryptochromes and radical-pair chemistry (Nordmann, Hochstoeger, and Keays 2022).

Magnetic modulation of cryptochrome signaling influences physiological and behavioral responses in several organisms (Gegear et al. 2010; Hore 2016). In plants, such modulation is increasingly interpreted within a broader framework of environmental signal integration, linking light perception, redox dynamics, hormonal signaling, and transcriptional regulation (Ahmad et al. 2016; Chaves et al. 2011).

Recent reviews emphasize growing consensus regarding the involvement of cryptochromes and radical-pair chemistry in plant magnetoreception (Thoradit et al. 2023; Nordmann, Hochstoeger, and Keays 2022). Within this framework, cryptochromes may function as integrative nodes that accumulate repeated redox perturbations and translate them into longer-term regulatory states.

Integrated transduction framework

Taken together, our results from cumulative correlations (Fig. 1), driver dominance spectra (Fig. 2), and multivariate robustness analyses (Fig. 3) support a hierarchical transduction pathway linking solar forcing to photosynthetic regulation. Solar variability modulates radiative and particle fluxes, which are transformed by the magnetosphere into geomagnetic disturbances. These disturbances interact with redox-active cofactors and radical-pair systems within chloroplasts, subtly perturbing PSI and b6f electron-transfer dynamics. The sensitivity of plants to such weak magnetic perturbations is supported by a substantial body of experimental evidence (Galland and Pazur 2005; Belyavskaya 2004; Parmagnani and Maffei 2022). The resulting redox imbalances promote ROS production and activate regulatory signaling pathways. Through cryptochrome-mediated and redox-sensitive networks, these signals are integrated over time and drive sustained adjustments in photosystem stoichiometry, energy dissipation, and carbon assimilation.

This framework reconciles short-term physical interactions with long-term ecosystem-scale responses and provides a mechanistic basis for the observed cumulative and temperature-dependent structure of the geomagnetic signal.

An evolutionary hypothesis: geomagnetic field as biological information

Beyond immediate physiological mechanisms, our findings invite a broader evolutionary interpretation. The pervasive presence of magnetosensitive elements—Fe–S clusters, radical-pair intermediates, and cryptochromes—across diverse taxa suggests that magnetic sensitivity may be an ancient and conserved feature of life (Imlay 2006; Rodgers and Hore 2009). Rather than evolving *de novo* in response to specific selective pressures, we propose that plants have co-opted pre-existing magnetosensitive components into regulatory networks that integrate multiple environmental signals.

This perspective shifts the interpretation of our observations: the cumulative, temperature-dependent response of SIF to geomagnetic disturbances reflects not a passive mechanical perturbation but an active biological perception. Plants appear to have evolved mechanisms to extract information from geomagnetic variability, much as they do from light, temperature, and water availability. The magnetosphere, in this view, functions as a dynamic mediator that transmits structured solar variability into the biosphere—a signal that plants have learned, over evolutionary time, to interpret.

Periods of geomagnetic instability, including polarity reversals and excursions, have been associated with major transitions in plant evolution and diversification (Meert et al. 2016; Glassmeier and Vogt 2009). While causal links remain speculative, such correlations are consistent with the hypothesis that magnetic variability has acted as a selective pressure, shaping the evolution of stress-response networks.

Within this framework, the observed suppression of SIF under geomagnetic disturbances represents not damage, but a regulated physiological adjustment—a recalibration of photosynthetic machinery in response to perceived environmental change. The cumulative nature of the response (Figs. 1, 3) suggests integration over time, a hallmark of biological information processing rather than simple physical insult.

This hypothesis generates testable predictions: (1) magnetically sensitive components should be embedded within broader stress-signaling networks; (2) the response should exhibit hallmarks of biological information processing, including adaptation, memory, and context-dependence; (3) organisms from lineages with different evolutionary histories should show different sensitivities, reflecting the selective pressures they have experienced.

Limitations and outlook

Our study is observational and cannot establish causality at the molecular level. Direct experimental tests using controlled magnetic-field manipulations and targeted measurements of PSI redox dynamics, ROS production, and cryptochrome signaling are required. Pioneering work on plant magnetoreception (Galland and Pazur 2005; Belyavskaya 2004) provides methodological frameworks for such experimental approaches. Improved mechanistic understanding will require coordinated laboratory, field, and satellite studies (Nordmann, Hochstoeger, and Keays 2022).

The molecular and biophysical foundations of magnetic-field effects in biological systems have been extensively discussed in recent reviews and theoretical analyses (Mattei and Hore 2014; Hore 2016; Thoradit et al. 2023). Integrating these advances with large-scale ecological observations represents a promising avenue for future research.

Conclusions

This study provides evidence that weak geomagnetic variability can become biologically relevant when filtered through temperature-dependent redox regulation in photosynthetic systems. The response is cumulative, temperature-dependent, and physiologically structured—hallmarks of biological information processing rather than passive mechanical perturbation.

Geomagnetic variability participates in photosynthetic regulation across multiple organizational levels, from short-term redox dynamics to long-term physiological acclimation. We propose that plants have evolutionarily co-opted geomagnetic signals as an informational layer of their environment, integrating them into existing redox-regulatory networks that govern stress responses. In this sense, geomagnetic forcing functions not merely as a physical perturbation, but as an evolved sensory input to which terrestrial vegetation has become functionally attuned.

The observed response implies that the magnetosphere may function not only as a physical shield but also as a dynamic mediator transmitting structured solar variability into biological regulation. Weak geomagnetic fluctuations, though energetically negligible, may become biologically effective precisely because they are interpreted through evolved sensory mechanisms rather than acting as direct physical agents. This perspective opens new frontiers in understanding

magnetosphere–biosphere coupling and suggests that the search for mechanisms should focus on regulatory networks, not merely on isolated physical effects.

5. Methods

The analytical strategy was designed to detect weak, cumulative biological signals embedded in strongly autocorrelated and environmentally driven time series. All methodological choices reflect this objective.

Data Sources and Processing

Geomagnetic variability was characterized using the Disturbance Storm Time index (Dst) from the OMNI2 dataset (Papitashvili and King 2020); see also (King and Papitashvili 2005) for details on solar wind data. We defined the Storm Intensity Index as $SII = -Dst$ to intuitively represent geomagnetic stress from a biological perspective. Solar activity was controlled using the F10.7 cm radio flux. Both indices were aggregated to daily means. To capture potential cumulative physiological effects alongside acute triggers, we computed both cumulative moving averages (1–90 days) and discrete time lags (1–90 days) for space weather indices.

Global SIF measurements were obtained from the OCO-2 Level 2 "Lite" datasets (V11r/V11.2r) (OCO-2 Science Team, Payne, and Chatterjee 2022). The OCO-2 instrument and its radiometric performance are described in detail by Crisp et al. (Crisp et al. 2017). We analyzed the 757/771 nm emission ratio (Stress Index) and individual emission lines aggregated to a daily $0.5^\circ \times 0.5^\circ$ grid. To minimize viewing geometry effects on SIF retrievals, we followed quality filtering recommendations (Sun et al. 2018) and applied strict thresholds for cloud and aerosol fractions. Strict quality filtering was applied based on MODIS (MCD12/MOD08) ancillary data (Myneni, Knyazikhin, and Park 2021): Cloud Fraction $< 60\%$, Aerosol Fraction $< 50\%$, and Leaf Area Index (LAI) ≥ 0.15. A 3×3 spatial dilation kernel was applied to the vegetation mask to minimize artifacts arising from grid mismatches between datasets.

To identify SIF anomalies, we fitted a seasonal trend model to each grid cell, accounting for linear trends and annual harmonic cycles. The resulting residuals were standardized using a Z-score transformation (SIF_{resid}) to ensure inter-variable comparability across different wavelengths and physiological indices.

Environmental controls (PAR, VPD, Temperature, Total Cloud Cover) were derived from ERA5 reanalysis (Hersbach et al. 2020, 2023) and resampled to the analysis grid. A critical distinction was made in the temporal treatment of environmental variables: unlike geomagnetic indices, environmental variables were primarily used to define the instantaneous physiological context and to isolate the specific contribution of space weather forcing.

Pairwise associations between geomagnetic and biospheric variables were quantified using Spearman's rank correlation, implemented as Pearson correlation applied to rank-transformed time series. Rank transformation makes the analysis robust to non-Gaussian noise and heavy tails typical of geophysical and remote-sensing residuals.

Multivariate Matrix Search

Simple pairwise correlations cannot distinguish genuine geomagnetic effects from indirect climatic covariation. To isolate the unique influence of geomagnetic activity from concurrent meteorological drivers, we implemented an exhaustive multivariate search using an Ordinary Least Squares (OLS) framework. We evaluated an exhaustive set of models spanning all combinations of integration windows for SII, PAR, and VPD:

$$SIF_{resid}(t) = \beta_0 + \beta_{SII} \cdot SII_{MA}(t, w_1) + \beta_{PAR} \cdot PAR_{MA}(t, w_2) + \beta_{VPD} \cdot VPD_{MA}(t, w_3) + \epsilon$$

Because the exhaustive regression grid produces heavily smoothed predictors and autocorrelated residuals, formal p-values in this setting should be interpreted cautiously. For the matrix search, we apply a computationally tractable effective-sample-size adjustment based on lag-1 autocorrelation of SIF residuals within each temperature bin. Extending the full multi-lag N_eff formulation to the entire regression grid would substantially increase computational complexity and is not warranted given that the matrix search is used here primarily as a robustness/effect-size diagnostic rather than a standalone hypothesis-testing framework.

Accordingly, primary statistical inferences regarding the existence, temperature dependence, and cumulative structure of the SII–SIF coupling are based on the correlation analyses with full autocorrelation and multiple-testing corrections,

while the matrix search serves to verify that the partial SII signal persists across a wide range of environmental window configurations.

This approach allowed us to calculate the partial regression coefficient (β_{SII}) and its associated t-statistic while rigorously controlling for light availability and vapor pressure deficit. The high-performance implementation enabled the processing of 10^9 model combinations, ensuring that the reported space-weather signals are not artifacts of environmental confounding.

While cumulative correlations were evaluated up to 90 days (on a sparse window grid), the multivariate matrix search was restricted to short windows (1–28 days; limited by collinearity and computational tractability). This restriction reduces collinearity between smoothed predictors and avoids inflated t-statistics in heavily overlapping long-window averages. This range captures the dominant physiologically relevant response timescale identified in the correlation analysis, while avoiding severe collinearity and computational intractability inherent to higher-dimensional regression at longer integration scales.

Importantly, the multivariate matrix search is not used here as a primary hypothesis-testing framework. Its purpose is to evaluate the robustness and biological plausibility of the geomagnetic signal under a wide range of environmental smoothing configurations, rather than to provide independent formal significance estimates.

All primary statistical inferences regarding the existence, temperature dependence, and cumulative structure of the SII–SIF coupling are based on the correlation analyses with rigorous autocorrelation and multiple-testing corrections. The matrix search therefore serves as a complementary diagnostic layer, designed to verify that the detected associations are not driven by specific model parametrizations or by indirect climatic covariation.

Temperature Stratification

The dataset was stratified into five physiological temperature bins based on the 10-day moving average of ambient temperature (T_{MA}): `Cold` ($T_{MA} < 10$°C), `Cool` (10°C $\leq T_{MA} < 19$°C), `Optimum` (19°C $\leq T_{MA} < 26$°C), `Warm Stress` (26°C $\leq T_{MA} < 31$°C), and `Extreme Heat` ($T_{MA} \geq 31$°C).

This stratification reflects established plant physiological thresholds, ranging from cold-induced metabolic limitation and excitation pressure (Sage and Kubien 2007; Ensminger, Busch, and Huner 2006; Huner, Öquist, and Sarhan 1998; Tikkanen and Aro 2014), through the broad photosynthetic optimum for C_3 vegetation (Yamori, Hikosaka, and Way 2014; Kumarathunge et al. 2019; Slot and Winter 2017), to progressive heat-induced impairment of Rubisco activity and electron transport (Crafts-Brandner and Salvucci 2000; Sharkey 2005; Allakhverdiev et al. 2008; Wahid et al. 2007).

This framework ensured that geomagnetic signals were evaluated within relatively stable physiological regimes, minimizing confounding by thermal stress.

Statistical Correction (N_{eff})

To account for temporal autocorrelation in geophysical time series, which inflates Type I error rates, we adjusted the effective degrees of freedom (N_{eff}) following Chelton (Chelton 1983) and the general formulation of Pyper and Peterman (Pyper and Peterman 1998). The effective sample size was estimated using the summed product of autocorrelation functions of the predictor (X) and response (Y):

$$N_{eff} = \frac{N}{1 + 2\sum_{k=1}^{K} r_X(k)\, r_Y(k)},$$

where $r_X(k)$ and $r_Y(k)$ denote lag-k autocorrelation coefficients, and K is the maximum lag considered. In practice, K was capped at 60 days (or N−2 for shorter series) to ensure numerical stability. Autocorrelation coefficients were computed on rank-transformed series to maintain consistency with the Spearman framework.

This multi-lag formulation accounts for enhanced autocorrelation induced by cumulative smoothing and prevents artificial inflation of statistical significance at long integration windows. The resulting N_{eff} values were used for all significance tests and confidence interval calculations.

To control for multiple hypothesis testing across integration windows within each temperature bin, p-values were adjusted using the Benjamini–Hochberg false discovery rate (FDR) procedure. This correction was applied separately for each driver and temperature regime.

Spatial Meta-Analysis

Global results were synthesized using an Inverse-Variance Weighting scheme (Cochran 1954). Local correlation coefficients were aggregated into regional means using inverse-variance weighting, with statistical precision approximated from N_{eff}-derived standard errors, ensuring robust estimation in sparse-data regions. To validate biological causality, we contrasted the signal strength in biological masks (`Control North`, `Global High-LAI`) against a non-biological negative control located in the Sahara Desert (`Sahara`). To differentiate between genuine biophysical responses and potential instrumental artifacts, we defined a `South Atlantic Anomaly` (SAA) scenario. The SAA is a region where the Earth's inner Van Allen radiation belt reaches its lowest altitude, exposing satellite sensors to increased fluxes of ionizing radiation and high-energy protons (Heirtzler 2002; Schaefer et al. 2016). For sun-synchronous spectrometers like OCO-2, these particles can induce transient "spikes" or increased dark current noise in the detectors (Crisp et al. 2017). By comparing the SIF-geomagnetic coupling in the SAA against radiation-stable regions (`Control North`), we assessed whether the observed signals were biologically grounded or driven by sensor-particle interactions. The map of the four regions is visualized in Supplementary Fig. S9.

Surrogate analysis

To test whether the observed cumulative association between SIF anomalies and geomagnetic activity could arise from autocorrelated temporal structure alone, we performed a surrogate analysis based on permutation of geomagnetic years.

Daily geomagnetic forcing was represented by the SII. For each surrogate realization, the daily SII time series was partitioned into calendar years and the yearly segments were randomly permuted. This procedure preserves the internal temporal structure of geomagnetic disturbances within individual years while disrupting the interannual phase alignment between the geomagnetic forcing and the biospheric response.

For each surrogate SII series, cumulative geomagnetic drivers were recomputed as moving averages over window lengths from 1 to 90 days, matching the windows used in the main analysis. Spearman correlations between SIF residuals and the surrogate cumulative SII series were then recomputed for all windows.

To summarize the correlation spectrum, we calculated the signed area under the curve (AUC) and the maximum absolute correlation within the biologically relevant window range of 20–30 days. Surrogate distributions of these statistics were obtained from 500 realizations, and empirical Monte-Carlo p-values were estimated using a +1 correction.

Code availability

All code necessary to reproduce the analyses and figures is available on Zenodo (DOI: 10.5281/zenodo.18715797).

Acknowledgements

We acknowledge use of NASA/GSFC's Space Physics Data Facility's OMNIWeb service and OMNI data. We thank the OCO-2 science team for providing the solar-induced fluorescence (SIF) data, available through the NASA Goddard Earth Sciences Data and Information Services Center (GES DISC). We acknowledge the European Centre for Medium-Range Weather Forecasts (ECMWF) for the ERA5 reanalysis data, generated using Copernicus Climate Change Service information. We also thank the NASA MODIS mission scientists and associated data processing teams (LP DAAC) for the ancillary land cover and atmospheric data used in this analysis. We acknowledge the use of DeepSeek, a large language model assistant, for help with code optimization, debugging, and improving the English language presentation of this manuscript.

References

Ahmad, Margaret, Paul Galland, Thorsten Ritz, Roswitha Wiltschko, and Wolfgang Wiltschko. 2016. "Magnetic Intensity Affects Cryptochrome-Dependent Responses in Arabidopsis Thaliana." *Planta* 244 (4): 955–62. https://doi.org/10.1007/s00425-016-2580-0.

Allakhverdiev, Suleyman I., Vladimir D. Kreslavski, Vyacheslav V. Klimov, Dmitry A. Los, Robert Carpentier, and Prasanna Mohanty. 2008. "Heat Stress: An Overview of Molecular Responses in Photosynthesis." *Photosynthesis Research* 98 (1–3): 541–50. https://doi.org/10.1007/s11120-008-9331-0.

Anderson, Jan M., Wah S. Chow, and Young-Il Park. 1995. "The Grand Design of Photosynthesis: Acclimation of the Photosynthetic Apparatus to Environmental Cues." *Photosynthesis Research* 46 (1): 129–39. https://doi.org/10.1007/BF00020423.

Apel, Klaus, and Heribert Hirt. 2004. "Reactive Oxygen Species: Metabolism, Oxidative Stress, and Signal Transduction." *Annual Review of Plant Biology* 55 (1): 373–99. https://doi.org/10.1146/annurev.arplant.55.031903.141701.

Atkin, Owen K., and Mark G. Tjoelker. 2003. "Thermal Acclimation and the Dynamic Response of Plant Respiration to Temperature." *Trends in Plant Science* 8 (7): 343–51. https://doi.org/10.1016/S1360-1385(03)00136-5.

Belyavskaya, N. A. 2004. "Ultrastructure and Calcium Balance in Meristem Cells of Pea Roots Exposed to Extremely Low Magnetic Fields." *Advances in Space Research* 34 (7): 1612–17. https://doi.org/10.1016/j.asr.2004.01.022.

Cendrero-Mateo, M. Pilar, A. Elizabete Carmo-Silva, Albert Porcar-Castell, Erik P. Hamerlynck, Shirley A. Papuga, and M. Susan Moran. 2015. "Dynamic Changes in the Relationship Between Photochemical Reflectance Index and Photosynthesis Under Light and Temperature Fluctuations." *Functional Plant Biology* 42 (7): 614–26. https://doi.org/10.1071/FP14287.

Chaves, Inês, Richard Pokorny, Martin Byrdin, Nathalie Hoang, Thorsten Ritz, Klaus Brettel, Lars-Oliver Essen, Gijsbertus T. J. van der Horst, Alfred Batschauer, and Margaret Ahmad. 2011. "The Cryptochromes: Blue Light Photoreceptors in Plants and Animals." *Annual Review of Plant Biology* 62: 335–64. https://doi.org/10.1146/annurev-arplant-042110-103759.

Chelton, Dudley B. 1983. "Effects of Sampling Errors in Statistical Estimation." *Deep Sea Research Part A. Oceanographic Research Papers* 30 (10): 1083–103. https://doi.org/10.1016/0198-0149(83)90013-1.

Cochran, William G. 1954. "The Combination of Estimates from Different Experiments." *Biometrics* 10 (1): 101–29. https://doi.org/10.2307/3001666.

Cosentino, Chiara, Tom Hiscock, Peter J. Hore, and Anne Giersch. 2019. "Cryptochromes as Potential Sensors of Weak Magnetic Fields in Biological Systems." *Open Biology* 9 (8): 190091. https://doi.org/10.1098/rsob.190091.

Crafts-Brandner, Steven J., and Michael E. Salvucci. 2000. "Rubisco Activase Constrains the Photosynthetic Potential of Leaves at High Temperature and CO2." *Proceedings of the National Academy of Sciences* 97 (24): 13430–35. https://doi.org/10.1073/pnas.230451497.

Crisp, D., H. R. Pollock, R. Rosenberg, L. Chapsky, R. A. M. Lee, F. A. Oyafuso, C. Frankenberg, et al. 2017. "The on-Orbit Performance of the Orbiting Carbon Observatory-2 (OCO-2) Instrument and Its Radiometrically Calibrated Products." *Atmospheric Measurement Techniques* 10 (1): 59–81. https://doi.org/10.5194/amt-10-59-2017.

Demmig-Adams, Barbara, and William W. III Adams. 1996. "The Role of Xanthophyll Cycle Carotenoids in the Protection of Photosynthesis." *Trends in Plant Science* 1 (1): 21–26. https://doi.org/10.1016/S1360-1385(96)80019-7.

Ensminger, Ingo, Florian Busch, and Norman P. A. Huner. 2006. "Photostasis and Cold Acclimation: Sensing Low Temperature Through Photosynthesis." *Physiologia Plantarum* 126 (1): 28–44. https://doi.org/10.1111/j.1399-3054.2006.00622.x.

Evans, E. W., and P. J. Hore. 2013. "Magnetic Field Effects in Biology from the Perspective of the Radical Pair Mechanism." *Journal of the Royal Society Interface* 10 (85): 20130499. https://doi.org/10.1098/rsif.2013.0499.

Foyer, Christine H., and Graham Noctor. 2005. "Oxidant and Antioxidant Signalling in Plants: A Re-Evaluation of the Concept of Oxidative Stress in a Physiological Context." *Plant, Cell & Environment* 28 (8): 1056–71. https://doi.org/10.1111/j.1365-3040.2005.01326.x.

Foyer, Christine, and Graham Noctor. 2009. "Redox Regulation in Photosynthetic Organisms: Signaling, Acclimation, and Practical Implications." *Antioxidants and Redox Signaling* 11 (4): 861–905. https://doi.org/10.1089/ars.2008.2174.

Frankenberg, Christian, Joshua B. Fisher, John Worden, Grayson Badgley, Sassan S. Saatchi, Jung-Eun Lee, Geoffrey C. Toon, et al. 2011. "New Global Observations of the Terrestrial Carbon Cycle from GOSAT: Patterns of Plant Fluorescence with Gross Primary Productivity." *Geophysical Research Letters* 38 (17): L17804. https://doi.org/10.1029/2011GL048738.

Galland, Paul, and Alexander Pazur. 2005. "Magnetoreception in Plants." *Journal of Plant Research* 118 (6): 371–89. https://doi.org/10.1007/s10265-005-0246-y.

Gegear, Robert J., Lauren E. Foley, Amy Casselman, and Steven M. Reppert. 2010. "Animal Cryptochromes Mediate Magnetoreception by an Unconventional Photochemical Mechanism." *Nature* 463 (7282): 804–7. https://doi.org/

10.1038/nature08719.

Glassmeier, Karl-Heinz, and Joachim Vogt. 2009. "The Earth's Magnetic Field and the Cretaceous Normal Superchron: A Review." *Space Science Reviews* 145 (3): 207–31. https://doi.org/10.1007/s11214-009-9534-1.

Guanter, Luis, Yongguang Zhang, Martin Jung, Joanna Joiner, Michael Voigt, Joseph A. Berry, Christian Frankenberg, et al. 2014. "Global and Time-Resolved Monitoring of Crop Photosynthesis with Chlorophyll Fluorescence." *Proceedings of the National Academy of Sciences* 111 (14): E1327–36. https://doi.org/10.1073/pnas.1320008111.

Heirtzler, J. R. 2002. "The Future of the South Atlantic Anomaly." *Journal of Atmospheric and Solar-Terrestrial Physics* 64 (16): 1701–8. https://doi.org/10.1016/S1364-6826(02)00120-7.

Hersbach, Hans, Bill Bell, Paul Berrisford, Gionata Biavati, András Horányi, Joaquín Muñoz Sabater, Julien Nicolas, et al. 2023. "ERA5 hourly data on single levels from 1940 to present." Accessed: 2025-11-05; Copernicus Climate Change Service (C3S) Climate Data Store (CDS). https://doi.org/10.24381/cds.adbb2d47.

Hersbach, Hans, Bill Bell, Paul Berrisford, Shoji Hirahara, András Horányi, Joaquín Muñoz-Sabater, Julien Nicolas, et al. 2020. "The ERA5 Global Reanalysis." *Quarterly Journal of the Royal Meteorological Society* 146 (730): 1999–2049. https://doi.org/10.1002/qj.3803.

Hore, Peter J. 2016. "The Radical Pair Mechanism and the Chemical Compass." *Biophysical Journal* 111 (12): 2519–25. https://doi.org/10.1016/j.bpj.2016.11.012.

Hore, Peter J., and Henrik Mouritsen. 2016. "The Radical-Pair Mechanism of Magnetoreception." *Annual Review of Biophysics* 45: 299–344. https://doi.org/10.1146/annurev-biophys-032116-094005.

Huner, Norman P. A., Gunnar Öquist, and Fathey Sarhan. 1998. "Energy Balance and Acclimation to Light and Cold." *Trends in Plant Science* 3 (6): 224–30. https://doi.org/10.1016/S1360-1385(98)01248-5.

Imlay, James A. 2006. "Iron-Sulphur Clusters and the Problem with Oxygen." *Molecular Microbiology* 59 (4): 1073–82. https://doi.org/10.1111/j.1365-2958.2006.05028.x.

Johnsen, Sönke, and Kenneth J. Lohmann. 2005. "The Physical Basis of Animal Magnetoreception: A Review." *Physics Today* 58 (3): 29–35. https://doi.org/10.1063/1.1897560.

King, J. H., and N. E. Papitashvili. 2005. "Solar Wind Spatial Scales in and Comparisons of Hourly Wind and ACE Plasma and Magnetic Field Data." *Journal of Geophysical Research* 110 (A2): A02104. https://doi.org/10.1029/2004JA010649.

Krieger-Liszkay, Anja. 2005. "Singlet Oxygen Production in Photosynthesis." *Journal of Experimental Botany* 56 (411): 337–46. https://doi.org/10.1093/jxb/eri037.

Kumarathunge, Dushan P., Belinda E. Medlyn, John E. Drake, Mark G. Tjoelker, Michael J. Aspinwall, Michael Battaglia, Francisco J. Cano, et al. 2019. "Acclimation and Adaptation Components of the Temperature Dependence of Plant Photosynthesis at the Global Scale." *New Phytologist* 222 (2): 768–84. https://doi.org/10.1111/nph.15668.

Kurisu, Genji, Huamin Zhang, Janet L. Smith, and William A. Cramer. 2003. "Structure of the Cytochrome B6f Complex of Oxygenic Photosynthesis: Tuning the Cavity." *Science* 302 (5647): 1009–14. https://doi.org/10.1126/science.1090165.

Mattei, Alessandro, and Peter J. Hore. 2014. "Magnetoreception: A New Role for the Radical Pair Mechanism?" *Biochemistry* 53 (5): 845–56. https://doi.org/10.1021/bi401495g.

Meert, Joseph G., Natalia M. Levashova, Mikhail L. Bazhenov, and Ed Landing. 2016. "The Role of Geomagnetic Field Intensity in Late Paleozoic Glaciation." *Geology* 44 (3): 183–86. https://doi.org/10.1130/G37522.1.

Meroni, M., M. Rossini, L. Guanter, L. Alonso, U. Rascher, R. Colombo, and J. Moreno. 2009. "Remote Sensing of Solar-Induced Chlorophyll Fluorescence: Review of Methods and Applications." *Remote Sensing of Environment* 113: 2037–51. https://doi.org/10.1016/j.rse.2009.05.003.

Mittler, Ron, Sandy Vanderauwera, Natsumi Suzuki, Gad Miller, Valeria B. Tognetti, Klaas Vandepoele, Martin Gollery, Vladimir Shulaev, and Frank Van Breusegem. 2011. "ROS Signaling: The New Wave?" *Trends in Plant Science* 16 (6): 300–309. https://doi.org/10.1016/j.tplants.2011.03.007.

Mohammed, G. H., R. Colombo, E. M. Middleton, U. Rascher, L. Nedbal, Y. Goulas, et al. 2019. "Remote Sensing of Solar-Induced Chlorophyll Fluorescence (SIF) in Vegetation: 50 Years of Progress." *Remote Sensing of Environment*. https://doi.org/10.1016/j.rse.2019.04.030.

Møller, Ian M., Poul Erik Jensen, and Anders Hansson. 2007. "Reactive Oxygen Species and Oxidative Signaling in Plant Mitochondria." *Physiologia Plantarum* 129: 56–64. https://doi.org/10.1111/j.1399-3054.2006.00803.x.

Müller, Patricia, Xiao-Ping Li, and Krishna K. Niyogi. 2001. "Non-Photochemical Quenching. A Response to Excess Light Energy." *Plant Physiology* 125 (4): 1558–66. https://doi.org/10.1104/pp.125.4.1558.

Munekage, Yuri, Maki Hashimoto, Chikahiro Miyake, Ken-Ichi Tomizawa, Tsuyoshi Endo, Masao Tasaka, and Toshiharu Shikanai. 2004. "Cyclic Electron Flow Around Photosystem i Is Essential for Photosynthesis." *Nature* 429

(6991): 579–82. https://doi.org/10.1038/nature02598.

Myneni, Ranga, Yuri Knyazikhin, and Taejin Park. 2021. "MODIS/Terra Leaf Area Index/FPAR 8-Day L4 Global 500m SIN Grid V061." Accessed: 2026-01-20; NASA EOSDIS Land Processes Distributed Active Archive Center (LP DAAC). https://doi.org/10.5067/MODIS/MOD15A2H.061.

Noctor, Graham, Jean-Philippe Reichheld, and Christine Foyer. 2018. "Reactive Oxygen Species, Antioxidant Networks and the Integration of Redox Signals in Plants." *Plant, Cell & Environment* 41 (10): 2257–72. https://doi.org/10.1111/pce.13186.

Nordmann, G. C., T. Hochstoeger, and D. A. Keays. 2022. "Magnetoreception in Plants: A New Field of Research?" *Trends in Plant Science* 27 (5): 423–26. https://doi.org/10.1016/j.tplants.2022.01.005.

OCO-2 Science Team, Vivienne H. Payne, and Abhishek Chatterjee. 2022. "OCO-2 Level 2 bias-corrected solar-induced fluorescence and other select fields from the IMAP-DOAS algorithm aggregated as daily files, Retrospective processing V11.2r." Accessed: 2025-12-31; NASA Goddard Earth Sciences Data; Information Services Center (GES DISC). https://doi.org/10.5067/8XXUQU7HBGBL.

Papitashvili, Natalia E., and Joseph H. King. 2020. "OMNI Hourly Data." Accessed: 2025-11-02; NASA Space Physics Data Facility. https://doi.org/10.48322/1shr-ht18.

Parmagnani, Ambra S., and Massimo E. Maffei. 2022. "Is the Radical Pair Mechanism Involved in the Magnetic Sensitivity of Plants?" *Plants* 11 (19): 2572. https://doi.org/10.3390/plants11192572.

Pfannschmidt, Thomas, Katharina Bräutigam, Raik Wagner, Lars Dietzel, Yvonne Schröter, Sabine Steiner, and Andriy Nykytenko. 2009. "Potential Regulation of Gene Expression in Photosynthetic Cells by Redox and Energy State: Approaches Towards Better Understanding." *Annals of Botany* 103 (4): 599–607. https://doi.org/10.1093/aob/mcn239.

Porcar-Castell, Albert, Esa Tyystjärvi, Jon Atherton, Christiaan van der Tol, Jaume Flexas, Erhard E. Pfuendel, Jose Moreno, Christian Frankenberg, and Joseph A. Berry. 2014. "Linking Chlorophyll a Fluorescence to Photosynthesis for Remote Sensing Applications: Mechanisms and Challenges." *Journal of Experimental Botany* 65 (15): 4065–95. https://doi.org/10.1093/jxb/eru191.

Pospíšil, Pavel. 2016. "Production of Reactive Oxygen Species by Photosystem II as a Response to Light and Temperature Stress." *Frontiers in Plant Science* 7: 1950. https://doi.org/10.3389/fpls.2016.01950.

Pyper, Brian J., and Randall M. Peterman. 1998. "Comparison of Methods to Account for Autocorrelation in Correlation Analyses of Fish Recruitment Data." *Canadian Journal of Fisheries and Aquatic Sciences* 55 (9): 2127–40. https://doi.org/10.1139/f98-104.

Rhoads, David M., and Chandra C. Subbaiah. 2006. "Mitochondrial Reactive Oxygen Species Production in Plants." *Plant Physiology* 141: 357–66. https://doi.org/10.1104/pp.106.078659.

Ritz, Thorsten, Salih Adem, and Klaus Schulten. 2000. "A Model for Photoreceptor-Based Magnetoreception in Birds." *Biophysical Journal* 78 (2): 707–18. https://doi.org/10.1016/S0006-3495(00)76629-X.

Ritz, Thorsten, Peter Thalau, John B. Phillips, Roswitha Wiltschko, and Wolfgang Wiltschko. 2004. "Magnetic Compass of Birds Is Based on a Molecule with Optimal Directional Sensitivity." *Biophysical Journal* 87 (4): 2673–80. https://doi.org/10.1529/biophysj.104.040774.

Rodgers, Christopher T., and Peter J. Hore. 2009. "Chemical Magnetoreception in Birds: The Radical Pair Mechanism." *Proceedings of the National Academy of Sciences* 106 (2): 353–60. https://doi.org/10.1073/pnas.0711966106.

Sage, Rowan F., and David S. Kubien. 2007. "The Temperature Response of C3 and C4 Photosynthesis." *Plant, Cell & Environment* 30 (9): 1086–106. https://doi.org/10.1111/j.1365-3040.2007.01682.x.

Samuilov, V. D., D. B. Bezryadnov, M. V. Gusev, A. V. Kitashov, and T. A. Fedorenko. 2001. "Hydrogen Peroxide Inhibits Photosynthetic Electron Transport in Cells of Cyanobacteria." *Biochemistry (Moscow)* 66 (6): 640–45. https://doi.org/10.1023/a:1010207314408.

Samuilov, V. D., A. Yu. Borisov, E. L. Barsky, O. F. Borisova, and A. V. Kitashov. 1998. "Quenching of Chlorophyll Fluorescence by Quinones." *Biochemistry and Molecular Biology International* 46 (2): 333–41. https://doi.org/10.1080/15216549800203842.

Schaefer, R. K., S. BenZvi, R. Caputo, et al. 2016. "Observation of the South Atlantic Anomaly with the Fermi Large Area Telescope." In *2016 IEEE Aerospace Conference*, 1–10. https://doi.org/10.1109/AERO.2016.7500768.

Sharkey, Thomas D. 2005. "Effects of Moderate Heat Stress on Photosynthesis: Importance of Thylakoid Reactions in Rubisco Deactivation." *Photosynthesis Research* 86 (3): 269–77. https://doi.org/10.1007/s11120-005-4367-1.

Shikanai, Toshiharu. 2014. "Central Role of Cyclic Electron Transport Around Photosystem i in the Regulation of Photosynthesis." *Current Opinion in Biotechnology* 26: 25–30. https://doi.org/10.1016/j.copbio.2013.08.012.

Slot, Martijn, and Klaus Winter. 2017. "In Situ Temperature Relationships of Biochemical and Stomatal Controls of

Photosynthesis in Tropical Trees." *Plant, Cell & Environment* 40 (11): 2354–65. https://doi.org/10.1111/pce.13048.

Sonoike, Kintake. 2011. "Photoinhibition of Photosystem i." *Physiologia Plantarum* 142 (1): 56–64. https://doi.org/10.1111/j.1399-3054.2010.01437.x.

Stroebel, David, Yves Choquet, Jean-Luc Popot, and Daniel Picot. 2003. "An Atypical Haem in the Cytochrome B6f Complex." *Nature* 426 (6965): 413–18. https://doi.org/10.1038/nature02155.

Sun, Ying, Christian Frankenberg, Jeffrey D. Wood, David S. Schimel, Martin Jung, Luis Guanter, Darren T. Drewry, et al. 2018. "OCO-2 Solar-Induced Chlorophyll Fluorescence: Characterization of the Valid SIF Retrieval and Its Dependence on Viewing Geometry." *Remote Sensing of Environment* 205: 231–43. https://doi.org/10.1016/j.rse.2017.11.025.

Suzuki, Nobuhiro, Shai Koussevitzky, Ron Mittler, and Gad Miller. 2006. "Reactive Oxygen Species and Temperature Stresses: A Delicate Balance Between Signaling and Destruction." *Physiologia Plantarum* 126 (1): 45–51. https://doi.org/10.1111/j.1399-3054.2006.00621.x.

Tapping, Kenneth F. 2013. "The 10.7 Cm Solar Radio Flux (F10.7)." *Space Weather* 11 (7): 394–406. https://doi.org/10.1002/swe.20064.

Thoradit, Tanate, Wuttichai Kamolsukyunyong, Thararat Srisurin, Nutchaya Sukhontasing, and Nontawat Pongsuchart. 2023. "Cryptochrome and Magnetic Sensing: A Review of the Current Evidence." *Journal of Plant Research* 136 (3): 295–308. https://doi.org/10.1007/s10265-023-01448-2.

Tikkanen, Mikko, and Eva-Mari Aro. 2014. "Integrative Regulatory Network of Plant Thylakoid Energy Transduction." *Trends in Plant Science* 19 (1): 10–17. https://doi.org/10.1016/j.tplants.2013.09.003.

Tiwari, Ashwani, Badri Raghuram, Gauri S. Singhal, and Anjana Jajoo. 2016. "Photoinhibition of Photosystem i Under Prolonged High Light Is Accelerated in the Absence of Alternative Electron Sink." *Physiology and Molecular Biology of Plants* 22 (3): 363–70. https://doi.org/10.1007/s12298-016-0372-8.

Wahid, Abdul, Saadat Gelani, Muhammad Ashraf, and Majid R. Foolad. 2007. "Heat Tolerance in Plants: An Overview." *Environmental and Experimental Botany* 61 (3): 199–223. https://doi.org/10.1016/j.envexpbot.2007.05.011.

Walters, Robin G. 2005. "Towards an Understanding of Photosynthetic Acclimation." *Journal of Experimental Botany* 56 (411): 435–47. https://doi.org/10.1093/jxb/eri060.

Way, Danielle A., and Wataru Yamori. 2014. "Diurnal Variation in the Temperature Response of Photosynthesis." *Plant Physiology* 166 (3): 1453–65. https://doi.org/10.1104/pp.114.247056.

Wiltschko, Roswitha, and Wolfgang Wiltschko. 2019. "Magnetoreception in Birds." *Journal of the Royal Society Interface* 16 (157): 20190295. https://doi.org/10.1098/rsif.2019.0295.

Xu, Jingjing, Lauren E. Jarocha, Tilo Zollitsch, Małgorzata Konowalczyk, Kevin B. Henbest, Sabine Moisan, et al. 2021. "Magnetic Sensitivity of Cryptochrome 4 from a Migratory Songbird Exhibits Species-Specific Properties." *Nature* 594 (7864): 535–40. https://doi.org/10.1038/s41586-021-03618-1.

Yamori, Wataru, Kouki Hikosaka, and Danielle A. Way. 2014. "Temperature Response of Photosynthesis in C3, C4, and CAM Plants: Temperature Acclimation and Temperature Adaptation." *Photosynthesis Research* 119 (1): 101–17. https://doi.org/10.1007/s11120-013-9874-6.